





# Fatigue Analysis of Vortex-Induced Vibration for Marine Risers with Top-End Platform Motion Excitations

Yuchao Yuan<sup>1,2</sup> , Hongxiang Xue<sup>1,2</sup> , Wenyong Tang<sup>1,2</sup>,  
and Jun Liu<sup>1,2</sup>

<sup>1</sup> State Key Laboratory of Ocean Engineering, Shanghai Jiao Tong University, Shanghai, China

{godyyyc, hongxiangxue, wytang, jliu}@sjtu.edu.cn

<sup>2</sup> Collaborative Innovation Center for Advanced Ship and Deep-Sea Exploration, Shanghai, China

**Abstract.** Vortex-induced vibration (VIV) of marine risers is a typical fluid-structure interaction (FSI) phenomenon. When considering the top-end platform motions, the nonlinearity of risers' VIV would strengthen significantly, making it become a worthwhile research frontier in ocean engineering. Platform heave leads to the riser's axial tension fluctuating with time varying (i.e. parametric excitation), while platform surge results in an equivalent unsteady flow field induced by the riser's forced oscillatory movements. To investigate the VIV response of a full-scale production riser with both platform heave and surge excitations, an alternative time domain numerical analysis procedure is established in this paper. The platform motion response is predicted with the help of three-dimensional potential flow theory, and the riser's VIV is simulated based on force-decomposition model. By updating the structural stiffness matrix and improving the VIV excitation force formula, the platform heave and surge excitations are taken into account respectively. Four types of cases including steady flow case, heave case, surge case and combined case are calculated to reveal their respective response characteristics as well as the coupling effect between the platform heave and surge excitations. Associated with rainflow counting algorithm and S-N curve method, the stress components of the riser's VIV under different cases are analyzed, and the structural fatigue damage is evaluated in detail. The obtained conclusions could provide some references to the engineering field at the design stage of marine risers.

**Keywords:** Marine risers · Vortex-induced vibration · Platform motion excitation · Response characteristic investigation · Fatigue damage evaluation

## 1 Introduction

With the oil and gas exploitation spreading to deeper sea, the safety of longer marine risers has been attracting increasing attention over the recent years. Vortex-induced vibration (i.e. VIV) is a fluid-structural interaction phenomenon commonly existing in ocean engineering, which is also a significant detrimental factor to the marine risers'

safety. When ocean current flows through, vortex would shed periodically around the riser, making the riser subjected to nonlinear hydrodynamic forces. As a flexible structure, the riser vibrates as a result of the oscillatory hydrodynamic forces, then disturbs the surrounding flow and corresponding hydrodynamic forces. More importantly, the vortex shedding may synchronize with the riser’s motion, and the response amplitude would enlarge evidently, causing severe fatigue damage even structural failure.

Under the actual marine environment, the encountered excitations of the riser are usually more complicated than most of the existing laboratory experiments and numerical simulations. Figure 1 is the sketch of platform-riser-seabed system under complicated marine environment. The riser is connected to the floating platform through the tensioner at top-end and its bottom is fixed at seabed. Due to wave and current load, the platform would experience diverse degrees of freedom motion response. Platform heave leads to the compression and stretch of the tensioner, then causing the axial tension of the riser fluctuating with time. The time-varying tension would affect the boundary condition and structural stiffness property of the riser. Platform surge drives the riser to oscillate in water, and the riser’s local oscillation amplitude decreases along the axial direction because of the bottom constraint. As a result, the riser would withstand an equivalent sheared-oscillatory flow field. Both the time-varying tension and equivalent unsteady flow have significant impacts on the riser’s dynamic analysis, therefore taking the platform motion excitations into consideration is necessary to achieve a deeper insight of the riser’s VIV response and fatigue characteristics under complicated marine environment.

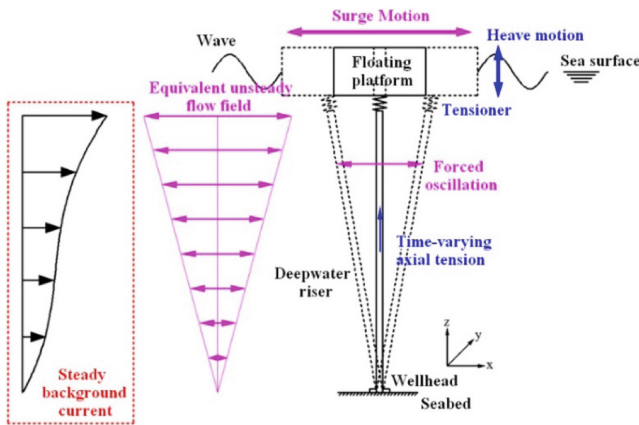


Fig. 1. Sketch of platform-riser-seabed system under complicated marine environment

Most of the existing experimental and numerical researches on risers’ VIV mainly focus on constant tension and steady flow cases. Over the last decades, the effects of time-varying tension and unsteady flow field on risers’ dynamic response are receiving increasing attention, and they have been investigated separately and preliminarily.

Franzini et al. [1] carried out the laboratory experiments of a 2.552 m riser's VIV with time-varying tension. Karniadakis et al. [2] made some efforts to investigate the VIV with varying structural bending stiffness with the help of spectral methods for computational fluid dynamics (CFD). Josefsson et al. [3] investigated the transverse VIV of a variable tension riser by combining CFD and computational structural dynamics (CSD) methods. There are also several alternative numerical models developed by da Silveira et al. [4], Tang et al. [5], Yang et al. [6] and Chen et al. [7], in which VIV is mostly simulated with wake oscillator models. When it comes to unsteady flow cases, some relevant research work has been published as well. Fu et al. [8] investigated the VIV response features of a 4 m riser under oscillatory flows with laboratory experiments, and Wang et al. [9] discussed the VIV fatigue damage of a 23.71 m truncated steel catenary riser (SCR) riser model with its top-end heaving in still water. Chang et al. [10] predicted a riser's VIV under the unsteady flow generated by the platform heave motion. Thorsen et al. [11, 12] developed a semi-empirical prediction approach and compared their numerical results with the test measurements of a top-tensioned riser (TTR) and an SCR under oscillatory flows. Besides, the riser's VIV under pure oscillatory flow cases and uniform combined with oscillatory flow cases are simulated with CFD technique [13–15]. Above experimental and numerical researches all indicated that the time-varying tension and unsteady flow field induced by top-end platform motions both affects the riser's VIV response evidently.

The authors have developed a time domain numerical model available for riser's VIV prediction, and the prediction method has been validated against the published experimental results under time-varying tension cases and oscillatory flow cases respectively [16, 17]. As a subsequent research, the multi-degrees of freedom motion excitations of the top-end platform are taken into consideration simultaneously in this paper. The platform heave and surge motions are simulated as multi-frequency time-varying tension excitation and equivalent sheared-oscillatory flow field excitation respectively, so that a full-scale deepwater riser's VIV fatigue damage characteristics under complicated marine environment could be investigated in detail.

## 2 VIV Numerical Model Methodology

The adopted VIV numerical model in this paper has been published by the same authors before, so here just describe it briefly for the sake of conciseness, and more details could be found in Reference [16]. The time domain VIV prediction procedure is based on Euler-Bernoulli beam theory and force-decomposition model, and the hydrodynamic force coefficient database originates from the typical cylinder forced vibration experimental data [18]. If the structural dynamic response is out of the database range, an empirical hydrodynamic damping model proposed by Venugopal [19] will be used. The structural damping coefficient  $c_s$  is expressed as  $c_s = 4\pi m f \zeta$ , where  $m$  is the riser mass,  $f$  is the response frequency and  $\zeta$  is the structural damping ratio. The lock-in region is set as the non-dimensional frequency range of [0.125, 0.25]. When lock-in occurs, the riser element will be synchronized onto the structural natural frequency closest to the non-dimensional frequency of 0.17, which corresponds to the largest excitation force coefficient. A second-order digital control loop, consisting of a

phase error detector and a second-order tracker, is adopted to guarantee that the excitation force is truly in phase with the local velocity of the riser. The riser’s governing differential equation of motion is discretized in space by finite element method (FEM). The whole numerical model is based on direct-integration dynamic analysis, and the structural kinetic equation is solved with Hilber-Hughes-Taylor (HHT) method [20]. The VIV of marine risers is a typical fluid-structure interaction issue, with strong nonlinearity. Compared with explicit dynamic analysis, the implicit dynamic analysis usually shows better performance when solving such complicated mechanism issues due to its better convergence and stability.

This paper takes the multi-degrees of freedom motions of the top-end platform into consideration. Platform heave would lead to the time-varying axial tension of the riser, so the structural stiffness matrix is updated according to the real-time tension distribution at the beginning of each time step. Platform surge would force the riser’s top-end to oscillate in the original steady background current, causing an extra sheared-oscillatory flow field. Therefore, the VIV excitation force calculation is based on the time-varying velocity and direction of the complicated combined flow. The flow-chart of the riser’s VIV time domain analysis with platform motion excitations is shown in Fig. 2. Note that, the proposed numerical model has been well verified applicable for the VIV prediction of the marine risers under unsteady flow cases and time-varying tension cases in References [16, 17] respectively. It is reasonable to investigate the riser’s VIV response and fatigue characteristics with platform motion excitations based on the developed numerical analysis procedure.

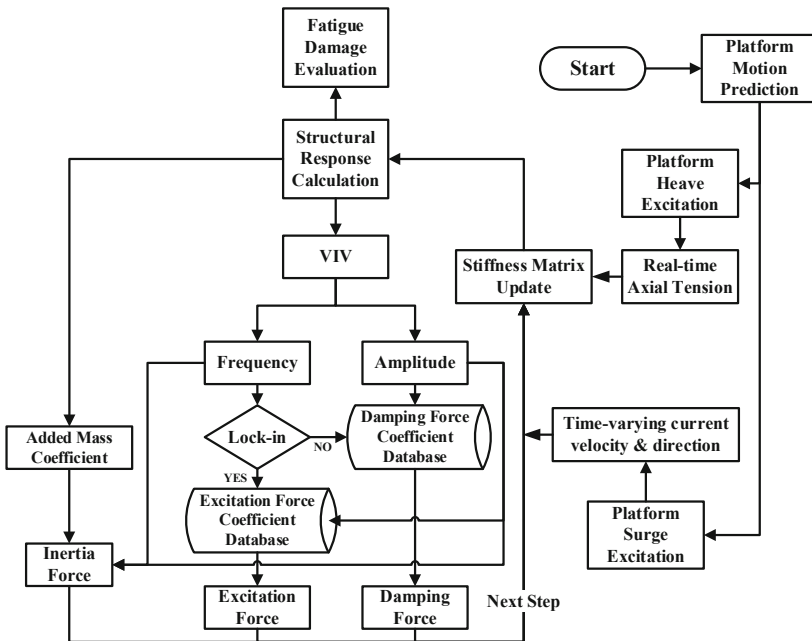


Fig. 2. Flow-chart of riser’s VIV time domain analysis with platform motion excitations

### 3 Top-End Platform Motion Excitations

To investigate the effect of the platform motion excitations on the riser's VIV, this section firstly predicts the time domain motion response of a tension leg platform (TLP) under the complicated marine environment, and then integrates the equivalent excitations of the top-end platform heave and surge into the riser's VIV analysis. Figure 3 shows the FE model of top-end platform for hydrodynamic calculation.

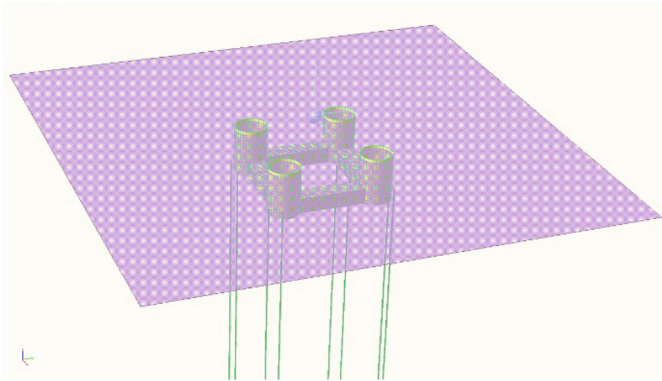


Fig. 3. FE model of TLP for hydrodynamic calculation

#### 3.1 Time Domain Motion Response Prediction

The motion response prediction of the top-end platform is based on three-dimensional potential flow theory and indirect time domain method. A TLP serving in 1500 m water depth is chosen, and its relevant parameters are listed in Table 1 and Table 2. There are eight tension legs connected with the floating platform to provide necessary constraint stiffness. The original length and outer diameter of the tension legs are 1474.04 m and 0.9235 m respectively, and the axial stiffness is 1968 t/m. The fixed point coordinate of tension legs at TLP is  $X = \pm 39.809$  m &  $Y = \pm 33.477$  m or  $X = \pm 33.477$  m &  $Y = \pm 39.809$  m, and the vertical position is 5.44 m. The main parameters of the TTR are shown in Table 3.

Table 1. Main parameters of TLP

Parameter	Value
Platform height from baseline (m)	54.0
Column height (m)	48.0
Draft (m)	28.0
Center distance between columns (m)	58.0
Column diameter (m)	20.0
Pontoon height (m)	9.5
Pontoon width (m)	10.72

**Table 2.** Parameters of TLP under work case

Parameter	Value
Water depth (m)	1500
Displacement (t)	51375.3
Total pretension of tension legs (t)	9160
Total pretension of top-tension risers (t)	4540.5
Platform weight (t)	37674.8
Gravity center height without TLs and TTR (m)	45.25
Inertia radius of roll without TLs and TTR (m)	33.20
Inertia radius of pitch without TLs and TTR (m)	33.72

**Table 3.** Main parameters of TTR

Parameter name	Value
Length (m)	1500
Outer diameter (m)	0.346
Inner diameter (m)	0.286
Young's modulus (GPa)	210
Poisson ratio	0.3
Wet mass per unit length (kg/m)	187.10
Axial stiffness (MN/m)	6196
Top-end pretension (t)	449.05

This paper selects the one-year-return-period sea state of China South Sea as the simulated marine environment. The parameters of the corresponding irregular wave are listed in Table 4. JONSWAP spectrum is chosen to describe the irregular wave, and the spectral shape parameter  $\gamma$  is taken as 3.3 for extremely deep water. Liu [21] gave the current profile distribution of South China Sea, as shown in Fig. 4.

**Table 4.** Parameters of irregular wave under one-year-return-period sea state

Parameter name	Value
Significant wave height (m)	8.7
Average zero-crossing period (s)	9.92
Spectral peak period (s)	12.30
Spectral peak frequency (rad/s)	0.51
Spectral peak magnitude ( $m^2s/rad$ )	20.77

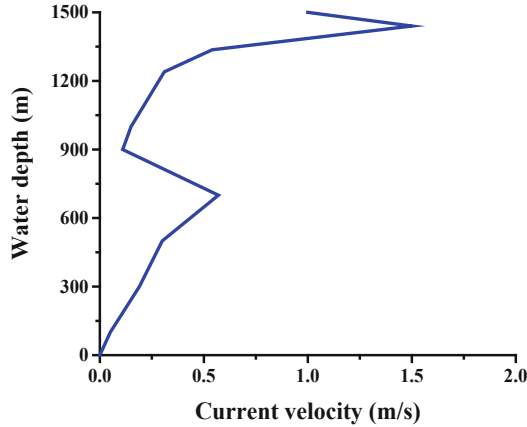


Fig. 4. Current profile distribution of South China Sea [21]

The hydrodynamic behaviors (including added mass coefficient, damping coefficient and load Response Amplitude Operator i.e. RAO) of the TLP are obtained from the frequency domain prediction. Then they are used to calculate the platform’s time domain motion response under combined current and irregular wave. The time histories of platform heave and surge are presented in Fig. 5 and Fig. 6, where only the dynamic components are included. The calculation time interval is set as 10800 s, which is long enough to minimize the effect of the randomness induced by the irregular wave spectrum.

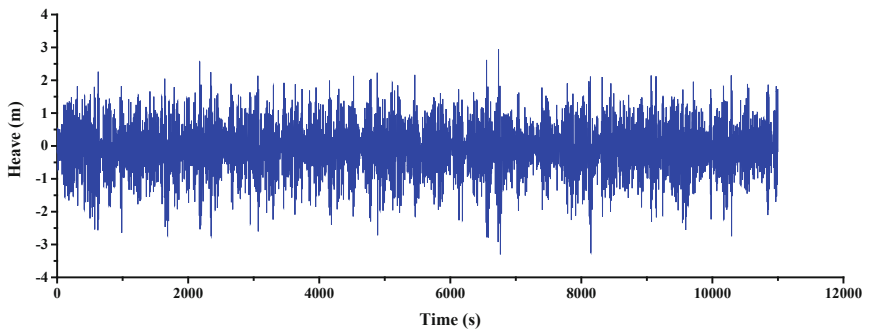


Fig. 5. Time history of TLP heave displacement under one-year-return-period sea state

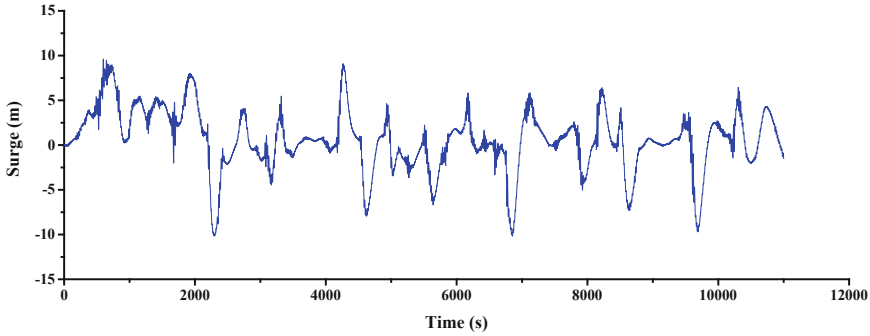


Fig. 6. Time history of TLP surge displacement under one-year-return-period sea state

### 3.2 Equivalent Excitation Simulation

The riser’s top-end is connected to the platform through the tensioner. The tension of the tensioner  $T$  is a function of the piston stroke  $s$ , approximately following the non-linear formula based on gas theory [22], as shown in Eq. (1).

$$T = \frac{T_0}{(1 + s/s_0)^c} \tag{1}$$

where  $T_0$  is the top-end pretension of the riser,  $s_0$  is the motion length interval of the piston,  $c$  is the gas constant which could be set as 1.0–1.3 according to the gas property of different types.  $s_0$  in this paper is taken as 11.2 m (down stroke  $s_{\text{down}} = -5.6$  m, and up stroke  $s_{\text{up}} = 5.6$  m), and  $c$  is set as 1.1. The relation curve between tension and stroke is shown in Fig. 7. Associated with the platform heave response in Fig. 5, the time history of the riser’s tension at top-end could be easily obtained, as shown in Fig. 8.

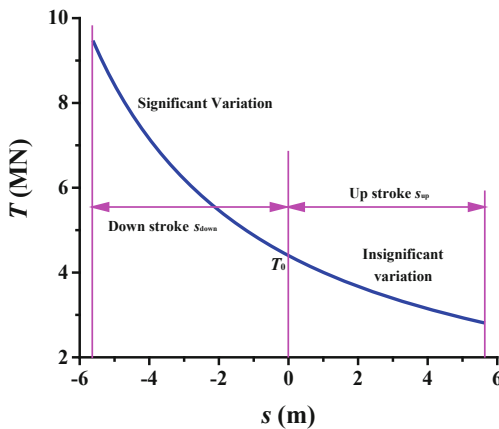
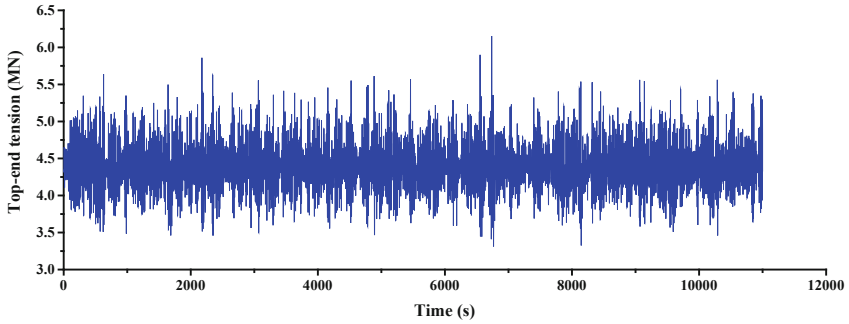


Fig. 7. Tension-stroke curve of tensioner





**Fig. 8.** Time history of deepwater riser top-end tension under one-year-return-period sea state

The combination of a sheared-oscillatory flow field is adopted to simulate the equivalent effect of the platform surge excitation. The derivation of the displacement time history in Fig. 6 with respect to time is obtained as shown in Fig. 9, which denotes the platform surge velocity. Based on the background steady flow, an extra sheared time-varying flow field, whose top-end velocity is equal to the platform instantaneous surge velocity, is included when predicting the riser's dynamic response. The rigid body swing movement of the riser induced by platform surge is taken into consideration so that the encountered velocity is always perpendicular to the riser's axial direction. The combined flow field presents obvious non-uniformity in both time and spatial domains.

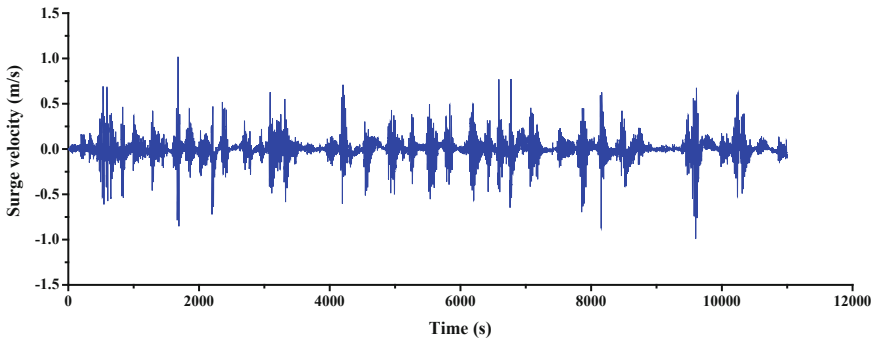


**Fig. 9.** Time history of riser's top-end equivalent velocity under one-year-return-period sea state

## 4 Dynamic Response Investigation

Four different types of load cases are simulated in this paper. Steady flow case only includes the steady background ocean current excitation, heave case includes the excitations of steady flow and platform heave motion, and surge case includes the excitations of steady flow and platform heave motion, while combined case includes the excitations of steady flow, platform heave as well as surge motions.

### 4.1 Local Response Characteristic

VIV displacement time histories at the riser's midpoint under four cases are shown in Fig. 10. VIV local response under steady flow case is relatively stable with visible periodicity, presenting the feature of the linear superposition of multi-frequency components. Above response features are similar with those under pure sheared flow cases. For the rest three cases, the nonlinearity of the displacement response is significant. Especially when  $t$  is around 700 s under heave case and when  $t$  is around 450 s under surge as well as combined cases, the riser presents different vibration processes from the adjacent time intervals. According to Fig. 9, there is obviously a sudden increase of the platform's surge velocity near  $t = 450$  s, which could explain the peak displacements at  $t = 450$  s for the Surge case and Combined case. Compared among the first three cases, the time-sharing and strongly nonlinear response characteristics induced by platform surge excitation are more evident than those induced by platform heave excitation. Figure 11 gives the VIV displacement amplitude spectra at the riser's midpoint under four cases. The first row follows the typical features under spatial non-uniform steady flow, i.e. multiple frequency peaks are excited discretely. Under heave case, some extra frequency components around the peak frequencies excited under steady flow case are also excited evidently. Associated with Reference [17], these weak but clearly existent frequencies are believed owing to the sub-harmonics induced by the axial multi-frequency parametric excitation. Under surge case, there is an apparent difference from steady flow case, i.e. the low-frequency components (less than 0.5 Hz) are excited additionally and the response energy concentrating at the dominant frequency of 0.7 Hz becomes much weaker. This is because the velocity variation range of the incoming current under surge case turns so broad that the riser would locate in the low-frequency response excitation region during some enough time intervals. While under combined case, the displacement amplitude spectrum covers the respective features of the first three cases. The sub-harmonic frequency components induced by platform heave excitation and the low-frequency response induced by platform surge excitation appear at the same time, and the dominant frequency of 0.7 Hz turns furtherly weaker.

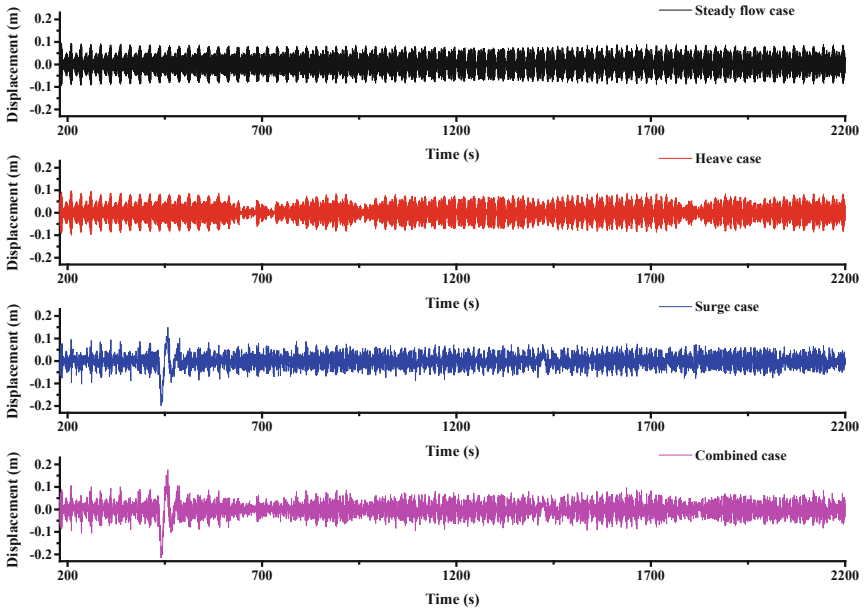


Fig. 10. VIV displacement time histories at the riser’s midpoint under four types of cases

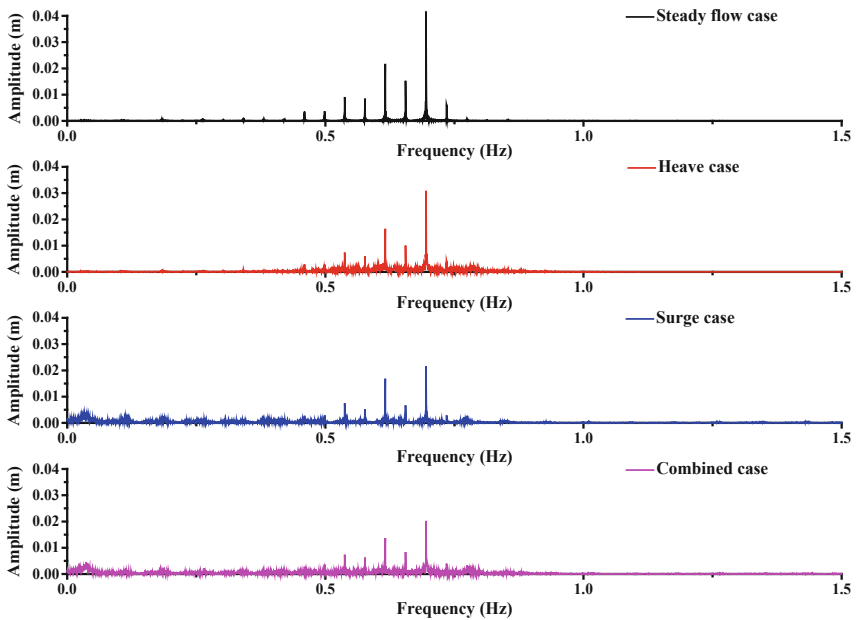


Fig. 11. VIV displacement amplitude spectra at the riser’s midpoint under four types of cases

### 4.2 Overall Response Characteristic

The envelopes of VIV maximum displacement along the riser under four cases are compared in Fig. 12. The envelopes of the first two cases are approximate, and heave case is a little larger than steady flow case within  $z/L$  between 0.45 and 0.82. When platform surge excitation is included, VIV maximum displacement enlarges obviously. In particular, the response amplitude could reach twice the corresponding values of steady flow case and heave case within the riser’s middle segment. The maximum displacement envelopes along the riser present lower order modal vibration shape than steady flow case and heave case as well. Under combined case, the maximum displacement is larger than pure heave or surge cases. It means the riser’s VIV response with multi-degrees of freedom platform motion excitations is more severe than that without or only with single-degree of freedom platform motion excitation. From the point of view in engineering application, the coupling aggravation effect between the platform’s different degrees of freedom motion excitations on the structural dynamic response should be taken into consideration for the riser’s stiffness design.

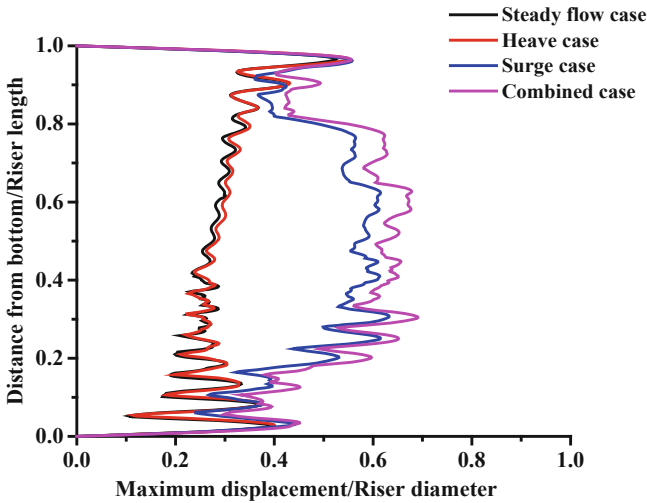


Fig. 12. Envelops of VIV maximum displacement along the riser under four types of cases

## 5 Fatigue Damage Evaluation

In this section, based on the predicted stress time history at the calculation location, the loop number of the alternating stress with different amplitudes is counted by rainflow counting algorithm. Then, the fatigue analysis of the deepwater riser with platform motion excitations is carried out with S-N curve method and Miner-Palmgren cumulative fatigue damage theory.

## 5.1 Stress Component Analysis

Figure 13 gives the envelopes of the maximum bending stress along the riser under four cases. Steady flow case and heave case have approximate stress level, and the maximum stress under surge case turns slightly larger, while the corresponding value reach peak for combined case. Above magnitude relation is quite similar with the maximum displacement in Fig. 12, which indicates again that the combination with platform heave and surge excitations tends to cause more severe riser stress level than steady flow case and single motion excitation cases. According to the envelop shape, steady flow case and heave case basically present the 18th mode dominating the riser's dynamic response, while once platform surge excitation is included under both surge and combined cases, the dominant modal order becomes not clear enough and irregular maximum stress distribution appears, which is because more frequency components are excited with current velocity variation range broadening.

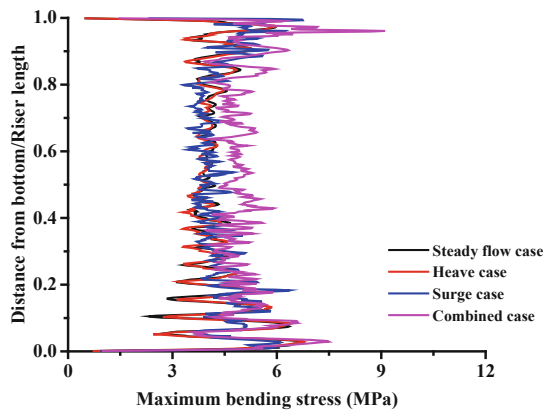


Fig. 13. Envelopes of maximum stress along the riser under four types of cases

Apart from the extreme stress level, the loop number of alternating stress would also importantly affect the structural fatigue damage. From Fig. 13, the response stress mainly fluctuates within [0 MPa, 10 MPa]. Here sets 0.2 MPa as a constant gradient to in turn count the loop number of the alternating stress with different amplitudes among [0 MPa, 0.2 MPa], [0.2 MPa, 0.4 MPa], [0.4 MPa, 0.6 MPa] and so on by rainflow counting algorithm. Figure 14, Fig. 15 and Fig. 16 represent the statistic results at three different axial locations of  $z/L = 0.1$ , 0.3 and 0.5 respectively.

For above three different calculation locations, the statistic results present identical regularity, namely, the loop number of alternating stress decreases with the stress amplitude increasing. It means the alternating stress induced by VIV is mainly dominated by high-frequency and small-amplitude components. Four cases could be classified into two groups. The stress loop numbers under steady flow case and heave case (i.e. Group i) are basically approximate, which is also true for surge case and combined case (i.e. Group ii). Compared with Group i, Group ii has broader variation range of stress amplitude. The loop numbers of small-amplitude alternating stress are larger and the ones of large-amplitude stress are smaller. For Group ii, although the

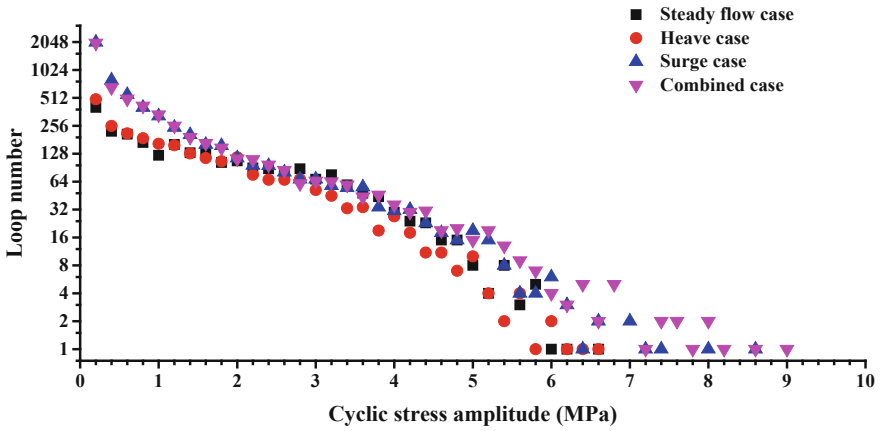


Fig. 14. Bending stress loop number of different loop stress amplitudes at  $z = 150$  m

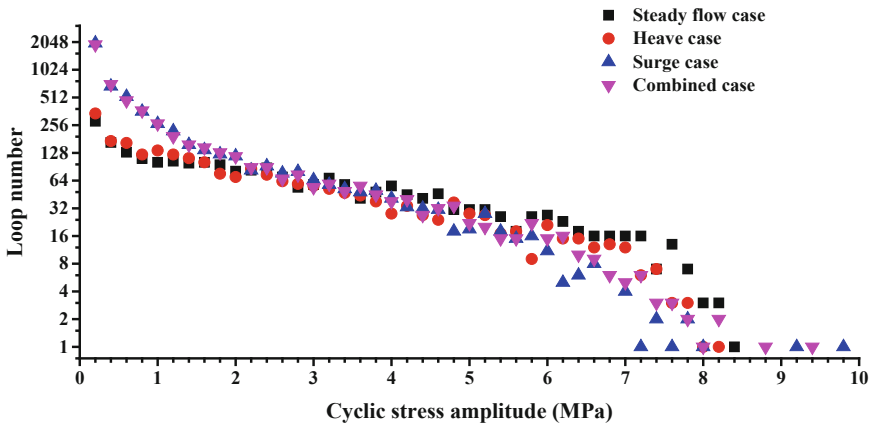


Fig. 15. Bending stress loop number of different loop stress amplitudes at  $z = 450$  m

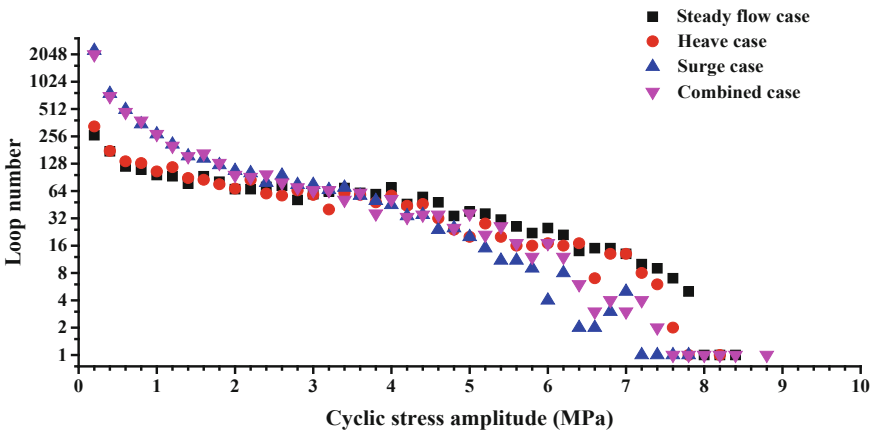


Fig. 16. Bending stress loop number of different loop stress amplitudes at  $z = 750$  m

large-amplitude alternating stress that causes larger fatigue damage single time has less loop number than Group i, the small-amplitude stress have much more loops which might also lead to larger structural damage. Therefore, which group has more severe total damage is still unknown before the cumulative fatigue analysis with S-N curve and Miner-Palmgren theory is carried out (Figure 15).

### 5.2 Fatigue Characteristic Comparison

The envelopes of VIV cumulative fatigue damage along the riser under four cases are shown in Fig. 17, where the relevant material parameters of the adopted S-N curve are taken as  $m = 3.0$  and  $A = 10^{11.687}$ . Steady flow case has the maximum fatigue damage, and heave case ranks the second, while the corresponding value of combined case is larger than surge case but smaller than heave case. Associated with the statistic results of the alternating stress loop number in Fig. 14, Fig. 15 and Fig. 16, it could be deduced that VIV fatigue damage is dominated by the large-amplitude stress components, namely, the case under which the large-amplitude alternating stress has more loops trends to accumulate more severe total structural damage. Compared to the three cases with platform motion excitations, the nonlinearity of VIV hydrodynamic forces under steady flow case is relatively weak, so the structural response is more stable, which is beneficial to accumulate fatigue damage. Note that, when the platform motion excitations come from single-degree of freedom to multi-degrees of freedom, the riser's fatigue damage may increase or decrease. In fact, the nonlinearity of load excitations under combined case is obviously stronger than heave case and surge case, causing the structural dynamic response being more unstable, so it acts as a detrimental role to accumulate severe fatigue damage. However, according to the maximum stress comparison in Fig. 13, the extreme stress response under combined case is larger than both heave case and surge case due to the coupling aggravation effect between the platform different degrees of freedom motion excitations, making the fatigue damage easier to enlarge. Who would dominate the final cumulative damage for the above two contradictory influence factors is still not clear enough under the condition that only single sea state is simulated in this paper.

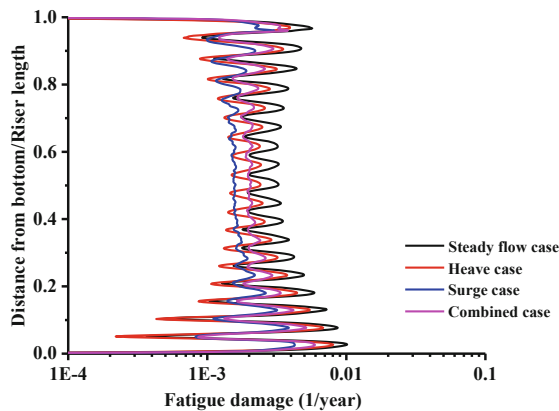


Fig. 17. Envelops of VIV fatigue damage along the riser under four types of cases

Compared with the results between four types of load cases, the effect of platform surge excitation on the riser's VIV fatigue analysis is much more significant than that of platform heave excitation. For a TLP, the heave stiffness provided by tension legs is usually large, which means platform heave amplitude is relatively smaller than its surge or sway response under the actual marine environment. So the parametric excitation induced by platform heave would not be very intensive. Moreover, platform surge excitation directly affects the riser's encountered current velocity as well as hydrodynamic forces, and VIV response is more sensitive to the obvious variation of flow field than the slight fluctuation of structural stiffness property. Therefore, it is reasonable that platform surge excitation has a stronger impact on the deepwater riser's fatigue characteristics.

## 6 Conclusion

An alternative time domain numerical model available for deepwater riser's VIV prediction in consideration of the top-end platform multi-degrees of freedom motion excitations is proposed in this paper. Firstly, the wave-induced motions of a TLP are predicted with three-dimensional potential flow theory. Secondly, platform heave excitation is simulated as the riser's time-varying tension, and platform surge excitation is equivalent to the unsteady combined flow field for the riser. Then, a full-scale marine riser's dynamic response is investigated under steady flow case, heave case, surge case and combined case. Finally, the riser's fatigue characteristics under four types of load cases are analyzed in detail. Some conclusions are drawn as follows.

(1) Under heave case, surge case and combined case, the nonlinearity of structural response displacement is significant, the response pattern changes with the variation of time and the amplitude modulates irregularly during the whole time interval. Compared with platform heave excitation, the nonlinear and time-sharing response characteristics of VIV with platform surge excitation are more apparent. Under combined case, both the sub-harmonic response induced by platform heave excitation and the low-frequency response induced by platform surge excitation occur simultaneously. The riser's VIV with platform multiple degrees of freedom motion excitations would be more intensive than that without or only with single degree of freedom motion excitation. Taking the coupling aggravation effect between the platform's different degrees of freedom motion excitations into account is necessary in the engineering design of marine risers.

(2) For the diverse components of VIV stress, the loop number of alternating stress decreases exponentially with the increase of stress amplitude. Compared with steady flow case and heave case, platform surge excitation would broaden the variation range of stress amplitude, increase the loop number of small-amplitude alternating stress and decrease the loop number of large-amplitude alternating stress under surge case and combined case.

(3) VIV fatigue damage is mainly dominated by the large-amplitude & low-frequency alternating stress among four types of cases. The fatigue damage under steady flow case is largest among all the four cases, followed by heave case, while the fatigue damage under combined case is larger than that under surge case but smaller than heave case. The effect of TLP heave excitation on riser's VIV fatigue damage is



relatively weaker than that of platform surge excitation. The magnitude relation between riser's VIV fatigue damage with single and multiple degrees of freedom motion of top-end platform is still unclear, and the direct calculation is necessary to effectively evaluate the structural cumulative fatigue damage.

Overall, this study would make efforts to promote the VIV response analysis and fatigue damage evaluation of the deepwater risers under complicated marine environment. The obtained conclusions could provide some references to the engineering design field. Under the actual marine environment, the encountered wave condition is more complicated than the simulated one by this paper, the long term probability distributions of wave direction as well as spectral shape parameter should also be taken into account. More detailed and further investigations need to be carried out in the future to precisely evaluate the deepwater riser's fatigue life with platform multi-degrees of freedom motion excitations.

**Acknowledgments.** This paper is based on the projects supported by the National Natural Science Foundation of China (Grant No. 51579146, 51490674) and Shanghai Rising-Star Program (Grant No. 16QA1402300).

## References

1. Franzini, G.R., Pesce, C.P., Gonçalves, R.T., Mendes, P., Fujarra, A.L.C.: Experimental investigations on Vortex-induced vibrations with a long flexible cylinder. Part II: effect of axial motion excitation in a vertical configuration. In: Proceedings of the 11th International Conference on Flow-Induced Vibration, The Hague, The Netherlands (2016)
2. Karniadakis, G.E., Sherwin, S.J.: Spectral/hp Element Methods for Computational Fluid Dynamics. Oxford University Press, New York, USA (2005)
3. Josefsson, P.M., Dalton, C.: Vortex-induced vibration of a variable tension riser. In: Proceedings of the 26th International Conference on Offshore Mechanics and Arctic Engineering, San Diego, California, USA, paper No. OMAE2007-29200 (2007)
4. da Silveira, L.M.Y., Martins, C.d.A., Leandro, D.C., Pesce, C.P.: An investigation on the effect of tension variation on VIV of risers. In: Proceedings of the 26th International Conference on Offshore Mechanics and Arctic Engineering. San Diego, California, USA. OMAE2007-29247 (2007)
5. Tang, Y.G., Shao, W.D., Zhang, J., Wang, L.Y., Gui, L.: Dynamic response analysis for coupled parametric vibration and vortex-induced vibration of top-tensioned riser in deep-sea. Eng. Mech. **30**(5), 282–286 (2013)
6. Yang, H.Z., Xiao, F.: Instability analyses of a top-tensioned riser under combined vortex and multi-frequency parametric excitations. Ocean Eng. **81**(2), 12–28 (2014)
7. Chen, W.M., Li, M., Guo, S.X., Gan, K.: Dynamic analysis of coupling between floating top-end heave and riser's vortex-induced vibration by using finite element simulations. Appl. Ocean Res. **48**, 1–9 (2014)
8. Fu, S.X., Wang, J.G., Baarholm, R., Wu, J., Larsen, C.M.: Features of vortex-induced vibration in oscillatory flow. J. Offshore Mech. Arct. Eng. **136**(1), 1–10 (2013)
9. Wang, J.G., Fu, S.X., Baarholm, R., Wu, J., Larsen, C.M.: Fatigue damage of a steel catenary riser from vortex-induced vibration caused by vessel motions. Marine Struct. **39**(39), 131–156 (2014)

10. Chang, S.H., Isherwood, M.: Vortex-induced vibrations of steel catenary risers and steel offloading lines due to platform heave motions. In: Proceedings of the Offshore Technology Conference. Houston, Texas, USA (2003)
11. Thorsen, M.J., Sævik, S., Larsen, C.M.: Time domain simulation of vortex-induced vibrations in stationary and oscillating flows. *J. Fluid Struct.* **61**, 1–19 (2016)
12. Thorsen, M.J., Sævik, S., Larsen, C.M.: Non-linear time domain analysis of cross-flow vortex-induced vibrations. *Marine Struct.* **51**, 134–151 (2017)
13. Zhao, M., Cheng, L., An, H.W.: Numerical investigation of vortex-induced vibration of a circular cylinder in transverse direction in oscillatory flow. *Ocean Eng.* **41**(5), 39–52 (2012)
14. Zhao, M., Kaja, K., Xiang, Y., Yan, G.R.: Vortex-induced vibration (VIV) of a circular cylinder in combined steady and oscillatory flow. *Ocean Eng.* **73**, 83–95 (2013)
15. Deng, Y., Huang, W.P., Zhao, J.L.: Combined action of uniform flow and oscillating flow around marine cylinder at low Keulegan-Carpenter number. *J. Ocean Univ. China* **13**(3), 390–396 (2014)
16. Yuan, Y.C., Xue, H.X., Tang, W.Y.: Numerical analysis of Vortex-Induced Vibration for flexible risers under steady and oscillatory flows. *Ocean Eng.* **148**, 548–562 (2018)
17. Yuan, Y.C., Xue, H.X., Tang, W.Y.: A numerical investigation of Vortex-Induced Vibration response characteristics for long flexible cylinders with time-varying axial tension. *J. Fluid Struct.* **77**, 36–57 (2018)
18. Gopalkrishnan, R.: Vortex induced forces on oscillating bluff cylinders. Doctoral thesis, Massachusetts Institute of Technology, Cambridge, USA (1993)
19. Venugopal, M.: Damping and response of a flexible cylinder in a current. Doctoral thesis, Massachusetts Institute of Technology, Cambridge, USA (1996)
20. Hilber, H.M., Hughes, T.J.R., Taylor, R.L.: Improved numerical dissipation for time integration algorithms in structural dynamics. *Earthq. Eng. Struct. Dyn.* **5**(3), 283–292 (1977)
21. Liu, H.: Concept design and analysis of deepwater drilling riser. Doctoral thesis, Harbin Engineering University, Harbin, China (2009)
22. Wang, K.P., Xue, H.X., Tang, W.Y.: Numerical simulation of hydropneumatic tensioner for coupled deepwater platform system. *J. Shanghai Jiao Tong Univ.* **46**(10), 1652–1657 (2012)